Design of dispersion-engineered As_2Se_3 channel waveguide for mid-infrared region supercontinuum generation

M. R. Karim,[1] H. Ahmad,[1,2,a)] Souvik Ghosh,[3] and B. M. A. Rahman[3]
[1)] *Photonics Research Centre, University of Malaya, 50603 Kuala Lumpur, Malaysia*
[2)] *Visiting Professor at the Department of Physics, Faculty of Science and Technology, Airlangga University, Surabaya 60115, Indonesia*
[3)] *Department of Electrical and Electronic Engineering, City University of London, Northampton Square, London, EC1V 0HB, UK*

(Dated: 3 May 2018)

In recent years, low cost and scalable integrated optics compatible planar waveguides have emerged for an ultrabroadband supercontinuum generation between ultraviolet and mid-infrared region applications. A 20-mm-long integrated photonics compatible highly nonlinear As_2Se_3 channel waveguide, which exhibited wider as well as lower magnitude and nearly flat anomalous dispersion region, designed and modeled by employing GeAsSe glass for its upper and lower claddings. Using pump source at 6 μm with a pulse duration of 170-fs, an ultrabroadband long wavelength region supercontinuum broadening covering the wavelength from 3.5 μm to up to 15 μm could be predicted with the largest input peak power of 10 kW. Further increasing power up to 20 kW does not enhance the supercontinuum expansion noticeably beyond 15 μm. This could be the longest supercontinuum generation by an on-chip integrated photonics compatible planar waveguide which can be used for a variety of mid-infrared region applications.

I. INTRODUCTION

Mid-infrared (MIR) supercontinuum (SC) sources made using integrated optics in the field of nonlinear optics in recent years have found quite essential in a variety of applications such as in MIR sensing and biomedical imaging[1]. Researchers are currently attempting to generate MIR SC covering the spectral region between 3 μm and 15 μm because almost all molecules in this region undergo strong vibrational absorption which is highly suitable for spectroscopy applications[2,3]. Microstructured fibers as well as planer waveguide geometries both are extensively investigated in recent years for expanding the SC spectra far into the MIR regime[4–10]. On-chip integrated optics devices have recently become famous for broadband SC generation owing to the nature of CMOS compatible devices[11]. As a platform of nonlinear optics, integrated circuit compatible photonics device using chalcogenide (ChG) glasses can be fabricated with high nonlinear parameter through combining its high Kerr nonlinearity and tight light mode confinement[12–15]. The high nonlinear parameter induced inside the ChG waveguide results in broadband SC spectral evolution extending up to the MIR[16,17]. In last decade, the main and popular approach was used to generate broadband SC from ultraviolet to near-infrared through microstructured based fibers designs[18]. The advantages of this approach are tight light mode confinement and controlled dispersion management that can be obtained through their structural parameter variations[19]. However, this approach is used to made with long interaction length which may result increased propagation loss and reduced shot to shot coherence over the entire SC output[20]. Planar waveguides alternative to the microstructured fibers, nowadays, are being considered for broadband SC sources design due to their short interaction length, scalable and low cost integrated optical chip fabrication[21–27].

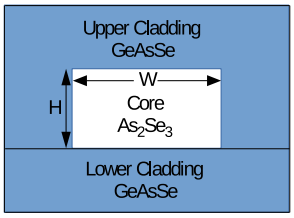

FIG. 1: Channel waveguide geometry.

To date, a few of the following longest wavelength theoretical and experimental SC spectral evolution were demonstrated through optical planar waveguide and fiber based designs[24–32]. Yu *et al.*[24] reported SC generation spanning up to the MIR covering the wavelength range 2 to 10 μm by an all-ChG rib waveguide using GeAsSe and GeAsS glasses for its upper and lower claddings, respectively, with 330-fs pulses pumped at 4.184 μm with an input peak power of 4.5 kW. Saini *et al.*[25] recently reported coherent MIR SC generation spanning from 1.2 to 7.2 μm numerically using a 2.5 mm long As_2Se_3 rib waveguide by pumping with 200-fs laser pulses at 2.8 μm with a peak power of 2.5 kW. In the same year, the authors numerically demonstrated SC generation in the MIR region using 6-mm long on-chip As_2Se_3 rib waveguide covering the wavelength ranges 1–10.9 μm and 1–11.88 μm for rectangular-core and triangular-core profiles using 497-fs pulses at 2.8 μm with a peak power of 6.4 kW[26]. The same group in the earlier year numerically reported MIR SC generation through 5-mm long on-chip $Ga_8Sb_{32}S_{60}$

[a)] Author to whom correspondence should be addressed: harith@um.edu.my

ChG rib waveguide spanning from 1 to 9.7 μm using a pump at 2.8 μm having a pulse duration of 497-fs with a peak power of 6.4 kW[27]. Using a 5-mm long triangular core graded index As_2Se_3 photonic crystal fiber, Saini *et al.*[28] have shown numerically the longest MIR SC expansion covering the spectral range 2 to 15 μm by employing pump at 4.1 μm with the largest peak power of 3.5 kW. Ou *et al.*[29] experimentally demonstrated a MIR region SC generation up to 14 μm with a 20-cm-long ChG step-index fiber made using $Ge_{15}Sb_{25}Se_{60}$ glass as the core and $Ge_{12}Sb_{20}Se_{65}$ glass for its cladding, pumped with a 150-fs pulse duration at 6 μm and a peak power of 750 kW. Cheng *et al.*[31] reported a SC spectral evolution up to the MIR covering the wavelength range 2 to 15.1 μm in a 3-cm-long ChG step-index fiber using As_2Se_3 as the core and employing $AsSe_2$ for its outer cladding pumped with a 170-fs pulses in 9.8 μm with a peak power of 2.89 MW. Zhao *et al.*[30] experimentally reported a MIR SC spectra expanding up to 16 μm using a 14-cm-long step-index fiber made from Ge-Te-AgI glass pumped with 150-fs pulses at 7 μm having a pulse repetition rate of 1 kHz with a peak power of 77 MW. Wang *et al.*[32] recently reported MIR region SC generation covering the wavelength from 2 to 12.7 μm using 12-cm long step-index fiber made using As_2Se_3 as a core and As_2Se_2S as an outer cladding by employing pump at 6.5 μm having pulses of 150-fs duration with a peak power of 93 MW.

In this paper, we propose a 20-mm-long channel waveguide and optimize it for pumping at 6 μm wavelength. The core of waveguide geometry is made with As_2Se_3 ChG glass which has excellent optical transparency in the range 0.85–17.5 μm among several ChG glass compounds with attenuation coefficient of less than 1/cm[36] and $Ge_{11.5}As_{24}Se_{64.5}$ ChG glass, which has taransparency up to 14 μm, is employed for both top and bottom claddings of the geometry. Moreover, this pair of glasses is thermally matched which is highly suitable for planar waveguide/step-index fiber fabrication[37]. Four different geometries are optimized through dispersion engineering by varying the waveguides dimensional parameters such as width and thickness. MIR region SC could be predicted beyond 15 μm by one of our proposed design and it would be, to the best of our knowledge, the longest MIR region SC spanning by a integrated photonics compatible planar waveguide design ever.

II. NUMERICAL MODEL

Figure 1 shows the our proposed planar geometry model in which As_2Se_3 and $Ge_{11.5}As_{24}Se_{64.5}$ glass materials are employed as core and cladding, respectively. The geometry was simulated using linear refractive index calculated through the following Selmeier equations that were reported for AsSe glass in[38] and for GeAsSe glass in[9].

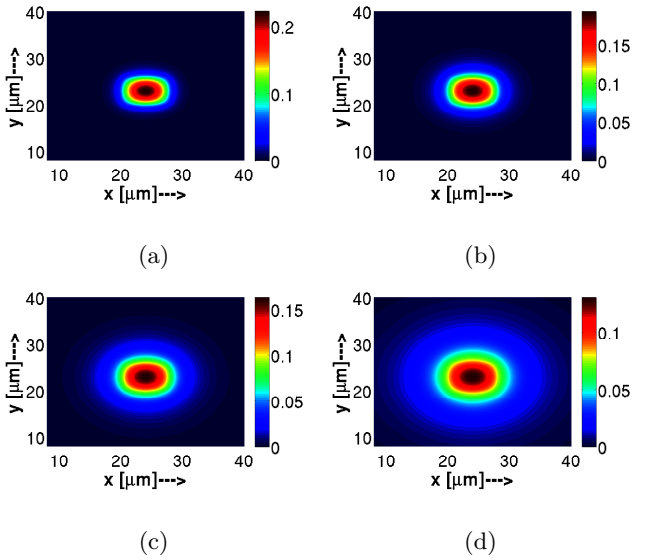

FIG. 2: Field profiles of fundamental TE polarized mode (H_y^{11}) are shown at a wavelength of (a) 6 μm; (b) 9 μm; (c) 12 μm; and (d) 15 μm for the waveguide structure of $H = 6$ μm and $W = 8$ μm.

$$n^2_{\mathrm{AsSe}}(\lambda) - 1 = \frac{4.994872\lambda^2}{\lambda^2 - 0.24164^2} + \frac{0.120715\lambda^2}{\lambda^2 - 19^2} + \frac{1.712369\lambda^2}{\lambda^2 - 4\times 0.24164^2}, \quad (1)$$

$$n^2_{\mathrm{GeAsSe}}(\lambda) - 1 = \frac{5.78525\lambda^2}{\lambda^2 - 0.28795^2} + \frac{0.39705\lambda^2}{\lambda^2 - 30.39338^2}, \quad (2)$$

where λ is calculated in micrometers.

For pumping the model at 6 μm, four different geometries are optimized by varying its width (W) and thickness (H). Our in-house developed full-vectorial finite element analysis mode solver was used to calculate mode propagation constant for the fundamental quasi transverse electric (TE) mode (H_y^{11}) of the proposed waveguide[33]. To achieve high accuracy modal solutions, more dense mesh divisions utilized in the transverse directions of the geometry through using waveguide half-symmetry. Four field profiles of fundamental TE polarized mode at four different wavelengths between 3 μm and 15 μm of a certain geometry are shown in Fig. 2 which imply excellent mode fields confinement inside that waveguide.

The one dimensional generalized nonlinear Schrödinger equation[18,34] can be solved for predicting SC generation

using the reported waveguide:

$$\frac{\partial A}{\partial z}+\frac{\alpha}{2}A-\sum_{k\geq 2}^{16}\frac{i^{k+1}}{k!}\beta_k\frac{\partial^k A}{\partial T^k}=i\gamma\left(1+\frac{i}{\omega_0}\frac{\partial}{\partial T}\right)\times\left(A\int_{-\infty}^{\infty}R(T)\mid A(z,T-T')\mid^2 dT'\right), \quad (3)$$

where the slowly-varying pulse envelope, $A = A(z,T)$ moves in a retarded time frame with the group-velocity $1/\beta_1$ ($T = t - \beta_1 z$) and the kth-order dispersion parameter is defined as β_k ($k \geq 2$). The nonlinear parameter is expressed as $\gamma = n_2\omega_0/(cA_{\text{eff}})$, where n_2 is the nonlinearity of AsSe material at the pump frequency ω_0, c denotes the speed of light, and A_{eff} indicates the frequency dependent effective mode area. Material absorption (linear propagation) losses are included through α into the left-hand part of the equation.

The response function of intrapulse Raman scattering[34], which plays a crucial role during SC generation, can be included during simulations as

$$R(t) = (1 - f_{\text{R}})\delta(t) + f_{\text{R}}h_{\text{R}}(t), \quad (4)$$

$$h_{\text{R}}(t) = \frac{\tau_1^2+\tau_2^2}{\tau_1\tau_2^2}\exp\left(-\frac{t}{\tau_2}\right)\sin\left(\frac{t}{\tau_1}\right). \quad (5)$$

where the parameters of As_2Se_3 glass are expressed as $f_{\text{R}} = 0.148$, $\tau_1 = 23$ fs, and $\tau_2 = 164.5$ fs[35].

III. NUMERICAL RESULTS

The generation of SC and its expansion continued to the mid-infrared depends critically not only on optical confinement but also on proper GVD optimization of the optical waveguides. To generate efficient broadband SC, waveguides need to be pumped with a low GVD value, vicinity to the zero-dispersion wavelength (ZDW) in the anomalous dispersion regime[18]. To achieve SC expansion far into the MIR, optical waveguide has to be optimized in such a way that it can be pumped as much as in a long wavelength region depending on the pump souce availability in that region. To meet this objective, we optimize our proposed waveguide geometries for pumping it at 6 μm wavelength. Cheng *et al.*[31] shows that a tunable pump wavelength between 2.4 μm and 11 μm can be produced by difference frequency generator with a pulse width of 170-fs and a repetition rate of 1 kHz. To achieve ZDW near the pump source wavelength of a waveguide geometry, we initially optimize a structure by setting up its W and H as 7 μm and 5 μm, respectively. The corresponding group-velocity dispersion curve of this geometry is shown as solid black line in Fig. 3. Obtained GVD curve for a waveguide geometry considered above remains normal dispersion region over a wide frequency range. The long wavelength 2nd ZDW of this GVD curve

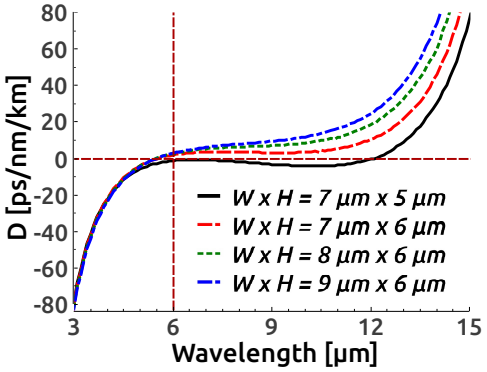

FIG. 3: GVD curves optimized for As_2Se_3 waveguide by varying W between 7 μm and 9 μm and H between 5 μm and 6 μm for pumping the waveguide at 6 μm.

can be observed beyond 12 μm and after that it crossed the GVD = 0 line and reached in anomalous dispersion regime. To obtain anomalous dispersion pumping GVD curve, we optimize a next structure by increasing waveguide H to 6 μm keeping W as same as before. Dashed-red line in Fig. 3 shows the corresponding GVD curve which is achieved with weak (low) GVD and nearly flat over a wide anomalous dispersion region. To observe the width sensitivity, keeping H fixed at 6 μm, we optimize two more geometries by enhancing W between 8 and 9 μm and their corresponding tailored GVD curves are shown as dotted-green and dashed-dotted blue lines in Fig. 3 as well. As seen in figure, the GVD curves of later designs follow the same pattern as earlier designs but keeping slightly moving up in the long wavelength side with increasing waveguide width.

For SC generation, our optimized waveguide geometries were simulated by solving the Eq. (1) with the symmetrized split-step Fourier method[34] using MATLAB. To accommodate extreme spectral broadening by avoiding negative frequency generation, the minimum tempo-

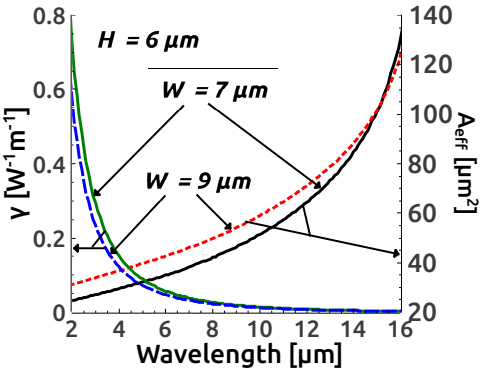

FIG. 4: For the waveguide geometry H = 6 μm and W = 7 μm or 9 μm, the mode effective areas and their corresponding nonlinear parameters are calculated over wide wavelength range.

ral resolution (time-step) was considered 10-fs by taking 2^{17} number of grid points during numerical simulations. The number of steps towards propagation direction were taken as 100,000 with a step size of 0.2 μm. To avoid spurious SC at the waveguide output, higher-order dispersion (HOD) terms up to 16$^{\text{th}}$ order (β_{16}) were included during all numerical simulations. Considering the nonlinear refractive index, $n_2 = 1.1\times10^{-17}$ m^2/W[15,19,31], Fig. 4 shows the calculated wavelength dependent nonlinear parameters from the mode-effective areas obtained through FEM mode-solver. As we could not able to obtain the linear propagation loss of As_2Se_3 glass in long wavelength edge for our proposed design, we have considered the constant absorption loss of 0.65 dB/cm which was reported in[36] for a mono-index As_2Se_3 glass fiber at 10.6 μm wavelength. We assume here more conservative linear absorption loss than the loss reported by Wang *et al.*[32] in their 12-cm long As_2Se_3 step-index fiber design for MIR region SC generation where they measured 4 dB/m average loss between 2.5 μm and 12 μm. The GVD values at pump wavelength for our proposed geometries are calculated from Fig. 3 as -3.26 ps/nm/km (solid-black line), 0.55 ps/nm/km (dashed-red line), 1.41 ps/nm/km (dotted-green line) and 1.64 ps/nm/km (dashed-dotted-blue line), respectively.

Initially, we consider waveguide structure $W = 7$ μm and $H = 5$ μm for SC generation. After evaluating and including HOD terms upto β_{16} from the GVD curve (solid-black line) obtained for this geometry in Fig. 3, SC simulations were carried out by launching a TE-polarized sech pulse with 170-fs duration into our optimized waveguide geometry for two different input peak power of 5 and 10 kW. Figure 5(a) shows the corresponding SC output covering the wavelength range 4.2–10.2 μm. The corresponding spectral density and spectrogram for an input power of 10 kW are shown in Fig. 6(a) and 7(a), respectively. In this case, as seen from figures that SC at waveguide output purely broadened only by self-phase modulation (SPM). As the pulse propagates in all-normal dispersion regime, SC spectrum does not extend sufficiently into the MIR due to the absence of soliton formation and hence soliton fission.

To pump our proposed waveguide in anomalous GVD region, we optimize next three geometries by varying width between 7 and 9 μm keeping thickness constant at 6 μm whose tailored wide anomalous dispersion region GVD curves are shown in Fig. 3. Soliton order, N, for these three geometries, can be calculated as $\sim$ 28, 17, 15 from the ratio of dispersion length (L_{D}) and nonlinear length (L_{NL}). Launching pump at 6 μm keeping other parameters same as before, SC can be expanded up to 12 μm as shown in Fig. 5(b) for the waveguide geometry having $W = 7$ μm. Spectral expansion beyond 15 μm can be predicted by increasing W to 8 μm which can be seen in Fig. 5(c). Along with SPM, here, SC broadening continues to the long wavelength as a result of wider region weak GVD as well as soliton fission and hence, it produces 17 fundamental solitons that are red-shifting owing

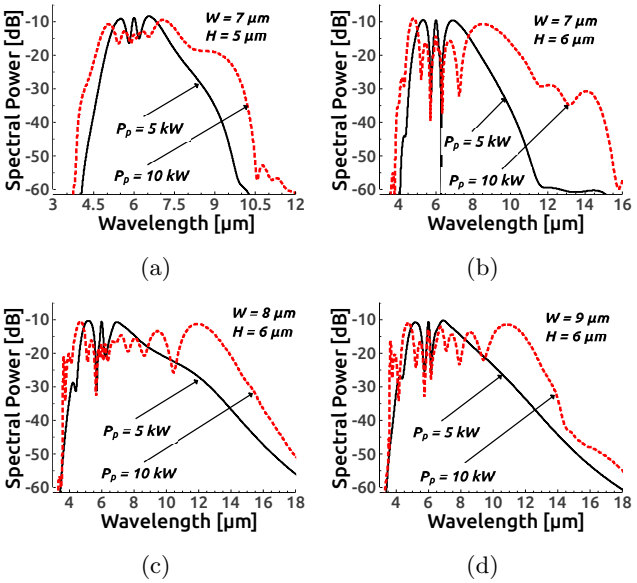

FIG. 5: SC spectra at the output of 20-mm-long waveguide (dimensional parameters as mentioned inside the figures) pumped at 6 μm using 170-fs pulses with 5 and 10 kW peak power. Four figures correspond to the GVD curves obtained in Fig. 3.

to the Raman induced frequency shift through Raman effect. A sharp and narrowband dispersive wave induces around at 3.5 μm of spectra which is located before the 1st ZDW of GVD curve in the normal dispersion region. SC bandwidth for all cases are measured at -20 dB point from the peak of the spectrum. By further increasing W to 9 μm, SC spectrum extended up to 14 μm as shown in

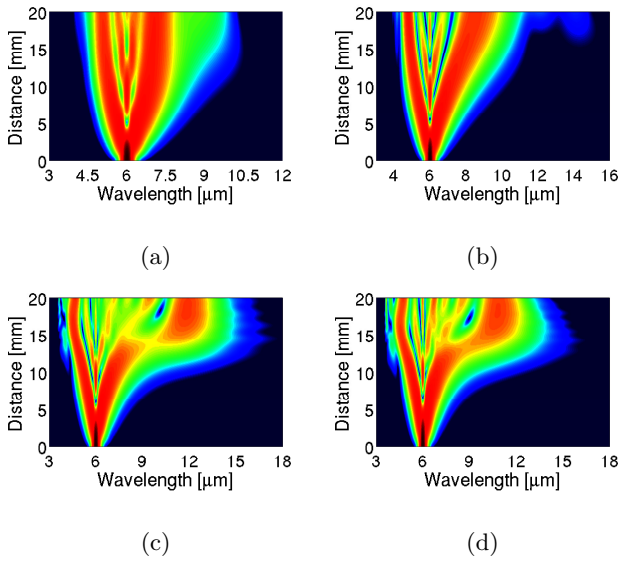

FIG. 6: Spectral density evolutions corresponding to the spectra obtained in Fig. 5 with an input peak power of 10 kW.

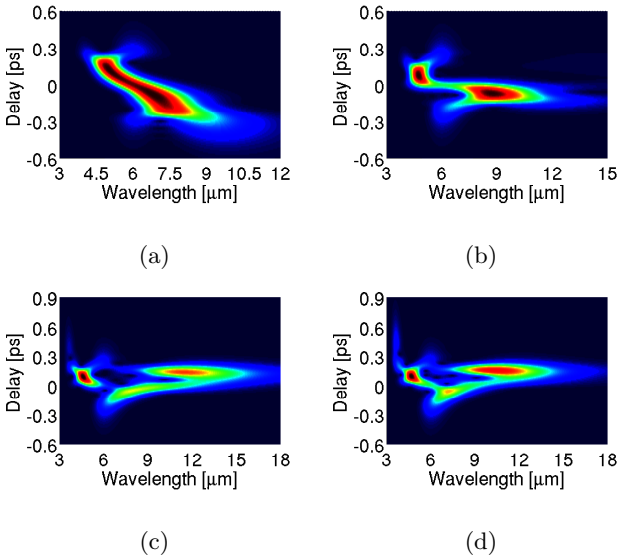

FIG. 7: Spectrograms corresponding to the spectra obtained in Fig. 5 with an input peak power of 10 kW.

Fig. 5(d) which is smaller than the bandwidth obtained in earlier design. The predicted SC expansions for the three geometries, which are analyzed above, can also be observed from spectral densities and spectrograms shown in Figs. 6(b)-6(d) and Figs. 7(b)-7(d), respectively. Thus, further increasing waveguide width shows spectrum reduces rather than expanding. By doubling peak power to 20 kW, we do not observe further expansion of SC bandwidth that can be seen in Fig 8 for the waveguide structure having $W = 8$ μm. As we have discussed before, the small GVD value over wide wavelength range in combination with waveguide nonlinearity results in large SC bandwidth at the waveguide output. In this case, further expansion of SC bandwidth beyond 15 μm is limited by the large GVD value which rises sharply after 15 μm

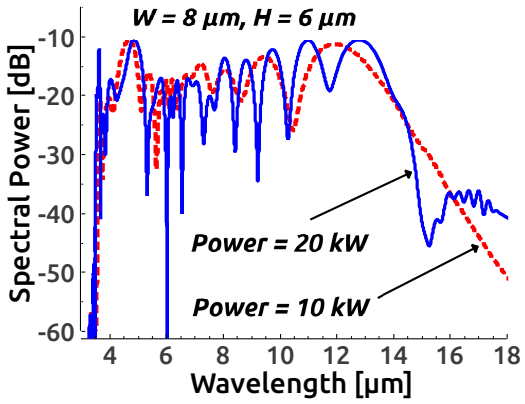

FIG. 8: SC spectra for the waveguide geometry of $H = 6$ μm and $W = 8$ μm at two different peak power 10 kW and 20 kW, respectively.

wavelength as can be seen in Fig. 3. Nevertheless, the largest expansion of MIR region SC up to 15 μm could able to be obtained by setting W at around 8 μm keeping $H = 6$ μm with a largest input peak power of 10 kW by our proposed channel waveguide design. However, as we have considered average material absorption loss, the SC bandwidth may eventually decreases somewhat at the waveguide output from the simulated values predicted at the output of our designs.

Until today, the widest MIR region SC generation, which is covered from 2 to 15 μm, has been demonstrated numerically by Saini *et al.*[23] where the authors optimized a 4 mm-long As_2Se_3 planar (rib) waveguide using MgF_2 and SiO_2 for its upper and lower claddings, respectively. Due to severe absorption loss of top and bottom claddings, the long wavelength extension of SC spectrum would be limited by this design. By our on-chip planar (channel) waveguide proposed in this paper, it may possible to obtain the longest SC extension beyond 15 μm with incurring tolerable cladding absorption in the long wavelength region.

IV. CONCLUSIONS

We have designed and optimized a number of 20-mm-long, dispersion-engineered, integrated optics compatible As_2Se_3 planar waveguides which can generate SC spectra far into the mid-infrared region up to 15 μm. The devices are designed suitably through the variations of their transverse dimensions such that they exhibit nearly flat anomalous dispersion profile with smaller magnitudes over a wide wavelength range. Considering and launching a femtosecond pump with pulses of 10 kW peak power at 6 μm wavelength, initially, all-normal dispersion but relatively flat SC broadening can be realized up to 10.2 μm by one of our optimized geometry with $H = 5$ μm and $W = 7$ μm. By increasing waveguide thickness, we obtain a wide anomalous dispersion GVD curve for a waveguide geometry of $H = 6$ μm and $W = 7$ μm. Spectrum can be extended up to 12 μm by this design. Next geometry is optimized by enhancing W to 8 μm keeping same H as earlier design as the GVD profile of the earlier design already reached in anomalous dispersion region with $H = 6$ μm. It has been realized through numerical simulation that SC broadening could able to be obtained beyond 15 μm by this design. Further increasing width does not extend the spectrum anymore rather than decreasing. Moreover, we do not observe any noticeable output SC bandwidth variation by increasing input peak power up to 20 kW.

Our As_2Se_3 planar waveguide model shows that it could be possible to obtain SC spectral broadening longer than 15 μm which is the broadest SC spectral evolution in the MIR regime and it may lead to new experimental activity to fabricate broadband integrated photonic device in this vital area for a variety of MIR region sensing and biological imaging applications.

ACKNOWLEDGEMENT

Funding for this research was provided by the Ministry of Higher Education (MOHE) under the grants LRGS (2015) NGOD/UM/KPT and the University of Malaya under the grant RP029A-15 AFR and RU001-2017.

[1] B. J. Eggleton, B. Luther-Davies, and K. Richardson, Chalcogenide photonics, Nat. Photonics **5**, 141–148 (2011).

[2] C. R. Petersen, U. Møller, I. Kubat, B. Zhou, S. Dupont, J. Ramsay, T. Benson, S. Sujecki, M. Abdel-Moneim, Z. Tang, D. Furniss, A. Seddon, and O. Bang, "Mid-infrared supercontinuum covering the 1.4-13.3 μm molecular fingerprint region using ultra-high NA chalcogenide step-index fiber," Nat. Photonics **8**, 830–834 (2014).

[3] A. Schliesser, N. Picque, and T. W. Haensch, "Mid-infrared frequency combs," Nat. Photonics **6**, 440–449 (2012).

[4] J. M. Dudley and J. R. Taylor, "Ten years of nonlinear optics in photonic crystal fiber," Nat. Photonics **3**, 85–90 (2009).

[5] K. Tajima, J. Zhou, K. Nakajima, and K. Sato, Ultra low loss and long length photonic crystal fiber, J. Lightwave Technol. **22**, 7–10 (2004).

[6] J. C. Knight and P. S. J. Russell, Photonic crystal fibers: New way to guide light, Science **296**, 276–277 (2002).

[7] J. C. Knight, T. A. Birks, P. S. Russell, and D. M. Atkin, All-silica single-mode optical fiber with photonic crystal cladding, Opt. Lett. **21**, 1547–1549 (1996).

[8] R. F. Cregan, B. J. Mangan, J. C. Knight, T. A. Birks, P. S. Russell, P. J. Roberts, and D. C. Allan, Single-mode photonic band gap guidance of light in air, Science **5433**, 1537–1539 (1999).

[9] P. Ma, D. Y. Choi, Y. Yu, X. Gai, Z. Yang, S. Debbarma, S. Madden, and B. Luther-Davies, "Low-loss chalcogenide waveguides for chemical sensing in the mid-infrared," Opt. Express **21**24, 29927–29937 (2013).

[10] M. R. Karim, B. M. A. Rahman, and G. P. Agrawal, "Dispersion engineered $Ge_{11.5}As_{24}Se_{64.5}$ nanowire for supercontinuum generation: A parametric study," Opt. Express **22**25, 31029–31040 (2014).

[11] D. Y. Oh, D. Sell, H. Lee, K. Y. Yang, S. A. Diddams, and K. J. Vahala, "Supercontinuum generation in an on-chip silica waveguide," Opt. Lett. **39**, 1046–1048 (2014).

[12] Y. Yu, X. Gai, T. Wang, P. Ma, R. Wang, Z. Yang, D. Choi, S. Madden, and B. Luther-Davies, "Mid-infrared supercontinuum generation in chalcogenides," Opt. Mater. Express **3**(8), 1075–1086 (2013).

[13] X. Gai, T. Han, A. Prasad, S. Madden, D. Y. Choi, R. Wang, D. Bulla, and B. Luther-Davies, Progress in optical waveguides fabricated from chalcogenide glasses, Opt. Express **18**, 26635–26646 (2010).

[14] M. R. E. Lamont, B. Luther-Davies, D. Y. Choi, S. J. Madden, and B. J. Eggleton, "Supercontinuum generation in dispersion engineered highly nonlinear ($\gamma = 10$ /W/m) As_2S_3 chalcogenide planar waveguide," Opt. Express **16**, 14938–14944 (2008).

[15] D. I. Yeom, E. C. Mägi, M. R. E. Lamont, M. A. F. Roelens, L. Fu, and B. J. Eggleton, "Low-threshold supercontinuum generation in highly nonlinear chalcogenide nanowires," Opt. Lett. **33**, 660-662 (2008).

[16] Y. Yu, B. Zhang, X. Gai, P. Ma, D. Choi, Z. Yang, R. Wang, S. Debbarma, S. J. Madden, and B. Luther-Davies, "A broadband, quasi-continuous, mid-infrared supercontinuum generated in a chalcogenide glass waveguide," Laser Photonics Rev. **8**, 1–7 (2014).

[17] M. R. Karim, B. M. A. Rahman, and G. P. Agrawal, "Mid-infrared supercontinuum generation using dispersion-engineered $Ge_{11.5}As_{24}Se_{64.5}$ chalcogenide channel waveguide," Opt. Express **23**5, 6903–6914 (2015).

[18] J. M. Dudley, G. Genty, and S. Coen, "Supercontinuum generation in photonic crystal fiber," Rev. Mod. Phys. **78**, 1135–1184 (2006).

[19] J. Fatome, C. Fortier, T. N. Nguyen, T. Chartier, F. Smektala, K. Messaad, B. Kibler, S. Pitois, G. Gadret, C. Finot, J. Troles, F. Desevedavy, P. Houizot, G. Renversez, L. Brilland, and N. Traynor, "Linear and nonlinear characterizations of chalcogenide photonic crystal fibers," J. Lightwave Technol. **27**11, 1707–1715 (2009).

[20] K. L. Corwin, N. R. Newbury, J. M. Dudley, S. Coen, S. A. Diddams, K. Weber, and R.S. Windeler, "Fundamental Noise Limitations to Supercontinuum Generation in Microstructure Fiber," Phys. Rev. Lett. **90**, 113904 (2003).

[21] J. M. Morris, M. D. Mackenzie, C. R. Petersen, G. Demetriou, A. K. Kar, O. Bang, and H. T. Bookey, "$Ge_{22}As_{20}Se_{58}$ glass ultrafast laser inscribed waveguides for mid-IR integrated optics," Opt. Mater. Express **8**, 1001–1011 (2018).

[22] N. Singh, D. D. Hudson, Y. Yu, C. Grillet, S. D. Jackson, A. Casas-Bedoya, A. Read, P. Atanackovic, S. G. Duvall, S. Palomba, B. Luther-Davies, S. Madden, D. J. Moss, and B. J. Eggleton, "Midinfrared supercontinuum generation from 2 to 6 μm in a silicon nanowire," Optica **2**, 797–802 (2015).

[23] T. S. Saini, A. Kumar, and R. K. Sinha, "Design and modelling of dispersion-engineered rib waveguide for ultra broadband mid-infrared supercontinuum generation." J. Modern Opt. **64** 143–149 (2016).

[24] Y. Yu, X. Gai, P. Ma, K. Vu, Z. Yang, R. Wang, D. Choi, S. Madden, and B. Luther-Davies, "Experimental demonstration of linearly polarized 2–10 μm supercontinuum generation in a chalcogenide rib waveguide," Opt. Lett. **41**5, 958-961 (2016).

[25] T. S. Saini, N. P. T. Hoa, K. Nagasaka, X. Luo, T. H. Tuan, T. Suzuki, and Y. Ohishi, "Coherent midinfrared supercontinuum generation using a rib waveguide pumped with 200 fs laser pulses at 2.8 μm," Appl. Opt. **57**, 1689–1693 (2018).

[26] T. S. Saini, U. K. Tiwari, and R. K. Sinha, "Design and analysis of dispersion engineered rib waveguides for on-chip mid-infrared supercontinuum," J. Lightwave Technol. **36**, 1993–1999 (2018).

[27] T. S. Saini, U. K. Tiwari, and R. K. Sinha, "Rib waveguide in Ga-Sb-S chalcogenide glass for on-chip mid-IR supercontinuum sources: Design and analysis," J. Applied Phy. **122**(5), 053104 (2017).

[28] T. S. Saini, A. Kumar, and R. K. Sinha, Broadband mid-infrared supercontinuum spectra spanning 2-15 μm using As_2Se_3 chalcogenide glass triangular-core graded-index photonic crystal fiber, J. Lightw. Technol. **33**, 3914–3920 (2015).

[29] H. Ou, S. Dai, P. Zhang, Z. Liu, X. Wang, F. Chen, H. Xu, B. Luo, Y. Huang, and R. Wang, Ultrabroad supercontinuum generated from a highly nonlinear GeSbSe fiber, Opt. Lett. **41**, 3201-3204 (2016).

[30] Z. Zhao, B. Wu, X. Wang, Z. Pan, Z. Liu, P. Zhang, X. Shen, Q. Nie, S. Dai, and R. Wang, Mid-infrared supercontinuum covering 2–16 μm in a low-loss telluride single-mode fiber, Laser Photonics Rev. **2**, 1700005 (2017).

[31] T. Cheng, K. Nagasaka, T. H. Tuan, X. Xue, M. Matsumoto, H. Tezuka, T. Suzuki, and Y. Ohishi, "Mid-infrared supercontinuum generation spanning 2 to 15.1μm in a chalcogenide step-index fiber," Opt. Lett. **41**, 2117–2120 (2016).

[32] Y. Wang , S. Dai, X. Han, P. Zhang, Y. Liu, X. Wang, and S. Sun, "Broadband mid-infrared supercontinuum generation in novel As_2Se_3-As_2Se_2S step-index fibers," Opt. Comm. **410**, 410-415 (2018).

[33] B. M. A. Rahman and J. B. Davies, "Finite-element solution of integrated optical waveguides," J. Lightwave Technol. **2**, 682–688 (1984).

[34] G. P. Agrawal, *Nonlinear Fiber Optics*, 5th ed. (Academic, Elsevier, 2013).

[35] L. Liu, T. Cheng, K. Nagasaka, H. Tong, G. Qin, T. Suzuki, and Y. Ohishi, "Coherent mid-infrared supercontinuum generation in all-solid chalcogenide microstructured fibers with all-normal dispersion," Opt. Lett. **41**2, 392–395 (2016).

[36] V. Shiryaev and M. Churbanov, "Trends and prospects for development of chalcogenide fibers for mid-infrared transmission, J. Non-Cryst. Solids **377**, 225–230 (2013).

[37]Z. G. Lian, Q. Q. Li, D. Furniss, T. M. Benson, and A. B. Seddon, "Solid microstructured chalcogenide glass optical fibers for the near- and mid-infrared spectral regions," IEEE Photonics Technol. Lett. **21**(24), 1804–1806 (2009).

[38]B. Ung and M. Skorobogatiy, "Chalcogenide microporous fibers for linear and nonlinear applications in the mid-infrared, Opt. Express **18**, 8647–8659 (2010).